Computation of Interphase Separation and Particle Fracture of Titanium Oxide/3003 Particle Reinforced Composites: The Role of Thermo-Mechanical Loading

[1]V. V. Satyanarayana and A. Chennakesava Reddy[2]

[1]Associate Professor, Department of Mechanical Engineering, Vasavi College of Engineering, Hyderabad, India
[2]Associate Professor, Department of Mechanical Engineering, Vasavi College of Engineering, Hyderabad, India
dr_acreddy@yahoo.com

Abstract: In the present work, the TiO_2/AA3003 alloy metal matrix composites were subjected to mechanical and thermal loads. The results obtained from the finite element analysis and experimental procedure of TiO_2/AA3003 alloy composites reveals the interphase separation from the particle and the matrix. Also, the particle fracture has been noticed in 30% TiO_2/AA3003 composites above 250^{o}C.

Keywords: Titanium oxide, AA3003 alloy, RVE model, finite element analysis, interphase separation, particle fracture.

1. INTRODUCTION

Interfaces are normally the weak link in metal matrix composites. Traditionally, material interphases are considered to exhibit tensile bond and shear resistance at the macroscopic continuum level. Simulating the phenomenon of interphase separation in composites has received a great deal of attention in recent years. At large deformations, particles tend to debond from the matrix, influencing both the ductility and fracture toughness of the composite. As a result of chemical interactions, an interphase may form between the particle and the matrix during manufacturing and processing. Even though these interphases are typically microscopic, they can greatly influence the macroscopic behavior of composite materials. The extent and composition of this interphase depends on a number of factors, including the surface area and surface treatment of the particles, as well as the level of mixing and age of the composite [1]. Debonding is characterized by a localized region of failure (or interfacial debonding) that accumulates around the particle inclusions. There have been numerous experimental investigations demonstrating the interfacial debonding behavior of particles under large deformations [2-10]. In two dimensions, the plain strain assumption is often employed to model fiber inclusions [11-15]. Zhong and Knauss [16] used linear softening cohesive elements to investigate debonding in fiber-reinforced composites with structured microstructures. They focused on the tensile response of the composites, and studied the influence of various factors; including particle size, shape and distribution.

The objective of the present paper was to evaluate the effect of thermo-mechanical loading on the interphase separation in titanium oxide/AA3003 alloy composites. The shape of titanium oxide nanoparticle considered in this work is spherical. The periodic particle distribution was a square array and corresponding representative volume element (RVE) is showed in figure 1.

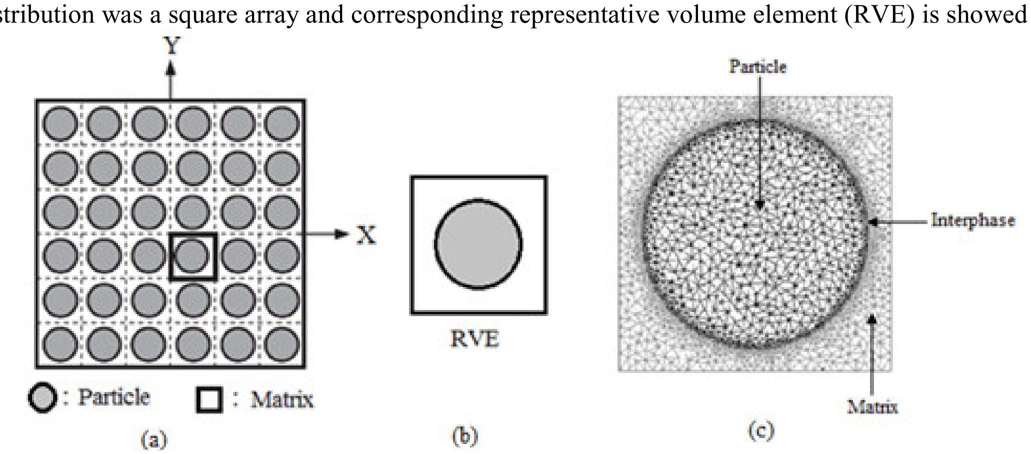

Figure 1: Square array of particles (a); Representative Volume Element (b); and Discretization of RVE (c).

2. MATERIALS METHODS

The matrix material was AA3003 alloy. The reinforcement material was titanium oxide (TiO_2) nanoparticles of average size 100nm. The mechanical properties of materials used in the present work are given in table 1.

Table 1: Mechanical properties of AA3003 matrix and TiO_2 nanoparticles

Property	AA3003	TiO_2
Density, g/cc	2.73	4.05
Elastic modulus, GPa	68.9	288.0
Coefficient of thermal expansion, 10^{-6} 1/°C	21.5	11.8
Specific heat capacity, J/kg/°C	893	697
Thermal conductivity, W/m/°C	163	11.8
Poisson's ratio	0.33	0.29

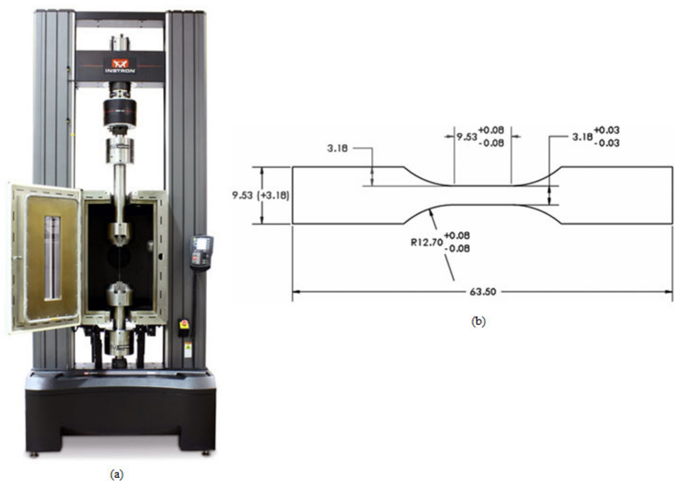

Figure 2: Tensile testing: UTM with temperature controlled chamber and (b) shape and dimensions of tensile specimen.

TiO_2/AA3003 alloy composites were fabricated by the stir casting process and low pressure casting technique with argon gas at 3.0 bar. The composite samples were give solution treatment and cold rolled to the predefined size of tensile specimens. The heat-treated samples were machined to get flat-rectangular specimens (figure 2) for the tensile tests. The tensile specimens were placed in the grips of a Universal Test Machine (UTM) with temperature controlled chamber at a specified grip separation and pulled until failure. The test speed was 2 mm/min. A strain gauge was used to determine elongation. In the current work, a cubical representative volume element (RVE) was implemented to analyze the tensile behavior TiO_2/AA3003 alloy composites at two (10% and 30%) volume fractions of TiO_2 and at different temperatures. The large strain PLANE183 element was used in the matrix in all the models. In order to model the adhesion between the matrix and the particle, a CONTACT 172 element was used.

3. RESULTS AND DISCUSSION

The optical micrograph as shown in figure 3 reveals random distribution of TiO_2 particles in AA3003 alloy matrix. Agglomeration of TiO_2 particles is also revealed in the microstructures.

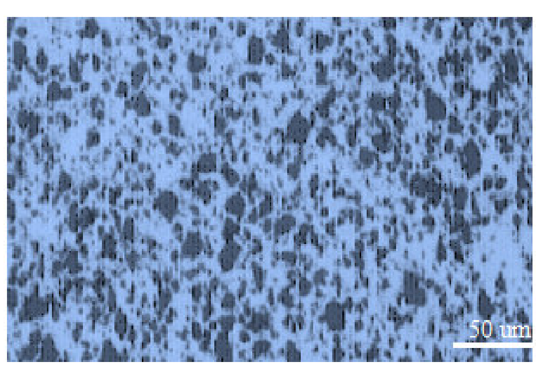

Figure 3: Microstructure showing distribution of 30%TiO_2 nanoparticles in AA3003 alloy matrix.

3.1 Thermo-Mechanical Behavior

Figure 4a shows the normalized elastic modulus of TiO_2/AA3003 composites at different temperatures. The elastic modulus is normalized with the elastic modulus of AA3003 alloy. The normalized elastic modulus is decreased with increase of temperature. Under thermo-mechanical loading, the stiffness of 30% TiO_2/AA3003 alloy composites is lower than that of 10% TiO_2/AA3003 alloy composites because of the difference in thermal properties of TiO_2 and AA3003 alloy. The normalized stiffness along the normal direction is lower than that along the load direction owing to tensile loading consideration in the present work. The normalized shear modulus increases with increase of temperature for 30% TiO_2/AA3003 but it is constant for 10% TiO_2/AA3003 as shown in figure 4b. The increase of major Poisson's ratio with temperature indicates the elongation along the load is greater than that along the transverse direction of loading of RVE (figure 4c).

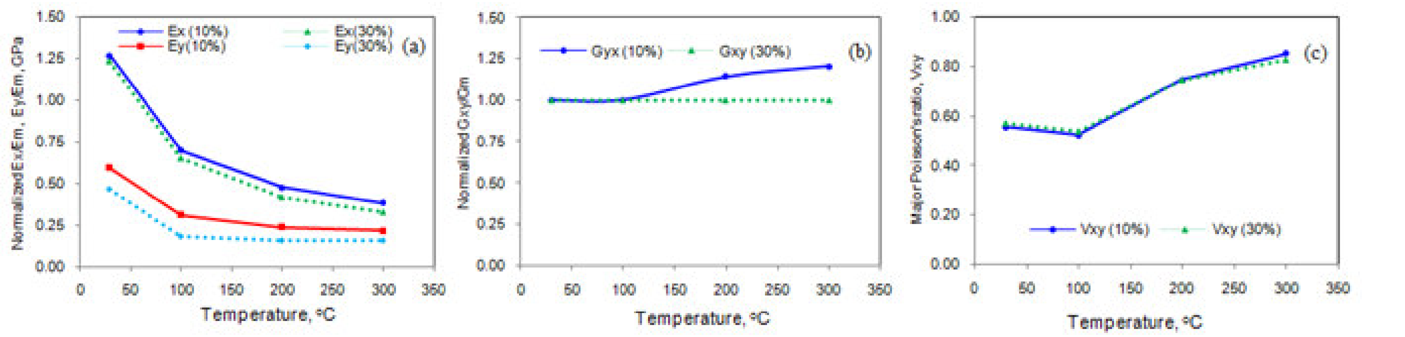

Figure 4: Effect of temperature on micromechanical properties of TiO_2/AA3003 composites.

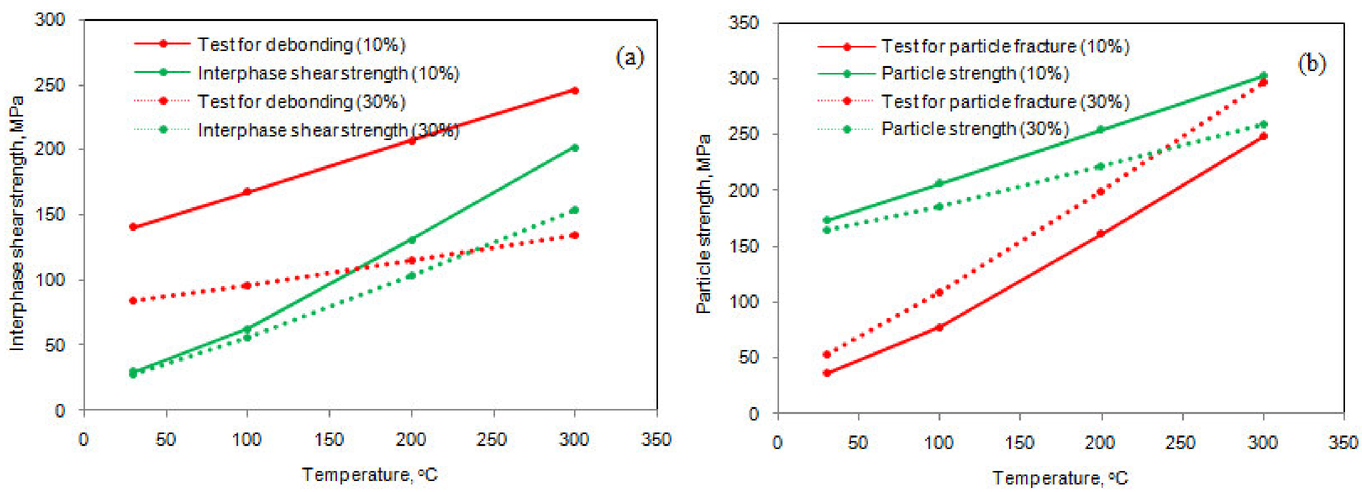

Figure 5: Criterion for interfacial debonding (a) and for particle fracture (b).

3.2 Fracture Behavior

If the particle deforms in an elastic manner (according to Hooke's law) then,

$$\tau = \frac{n}{2}\sigma_p \quad (1)$$

where σ_p is the particle stress. For the interfacial debonding/yielding to occur, the interfacial shear stress reaches its shear strength:

$$\tau = \tau_{max} \quad (2)$$

For particle/matrix interfacial debonding can occur if the following condition is satisfied:

$$\tau_{max} < \frac{n\sigma_p}{2} \quad (3)$$

It is observed from figure 5a that the interphase debonding occurs between TiO_2 nanoparticle and AA3003 alloy matrix as the condition in Eq.(3) is satisfied in 10%TiO_2/AA3003 composites while the interphase debonding occurs 250^{o}C in 30%TiO_2/AA3003 composites. The normal displacement field (figure 6) across the interphase increases with increase of temperature. This confirms the increase of interphase separation from TiO_2 particle and AA3003 alloy matrix with increase of temperature. Further, the normal and tangential tractions (figure 7) along the interphase increase with increase of temperature to take place the interphase separation from TiO_2 particle and AA3003 alloy matrix.

If particle fracture occurs when the stress in the particle reaches its ultimate tensile strength, $\sigma_{p,uts}$, then setting the boundary condition at

$$\sigma_p = \sigma_{p,\,uts} \tag{4}$$

The relationship between the strength of the particle and the interfacial shear stress is such that if

$$\sigma_{P,uts} < \frac{2\tau}{n} \tag{5}$$

Then the particle will fracture. From the figure 5b, it is observed that the TiO_2 nanoparticle was fractured above 250°C in 30%TiO_2/AA3003 composites only as the condition in Eq. (5) is satisfied. There was no TiO_2 particle fracture in 10%TiO_2/AA3003 composites.

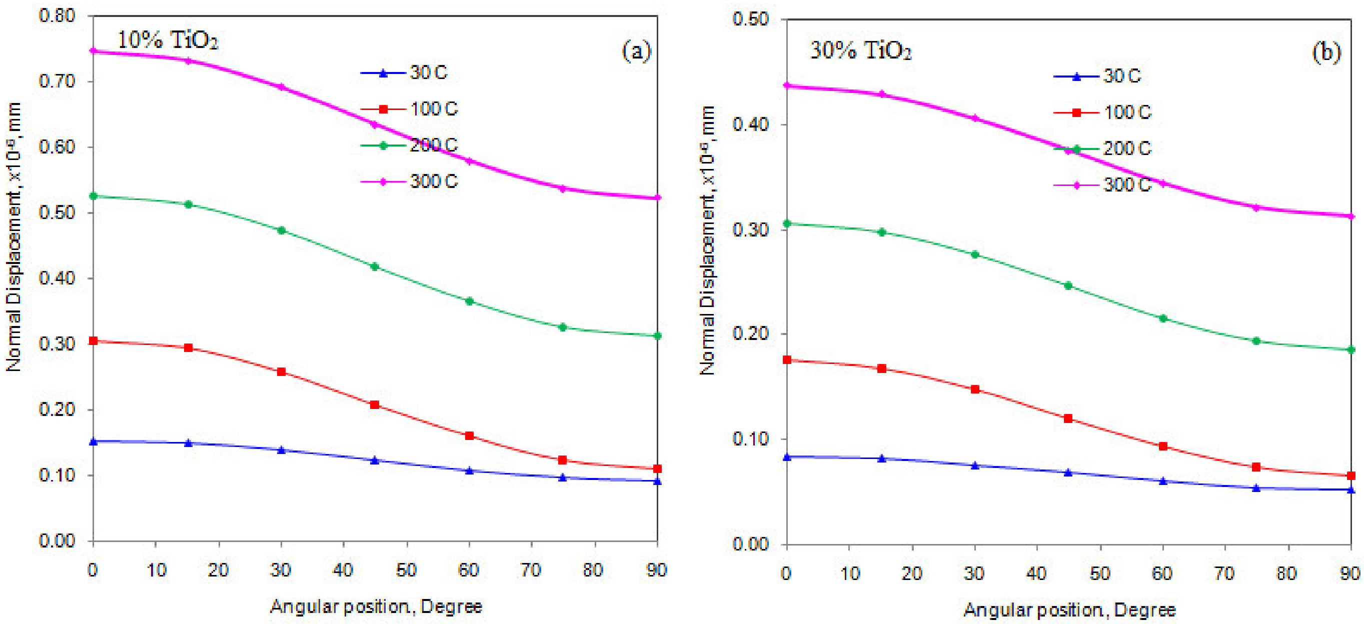

Figure 6: Normal displacement across the interphase between TiO_2 particle and AA3003 alloy matrix.

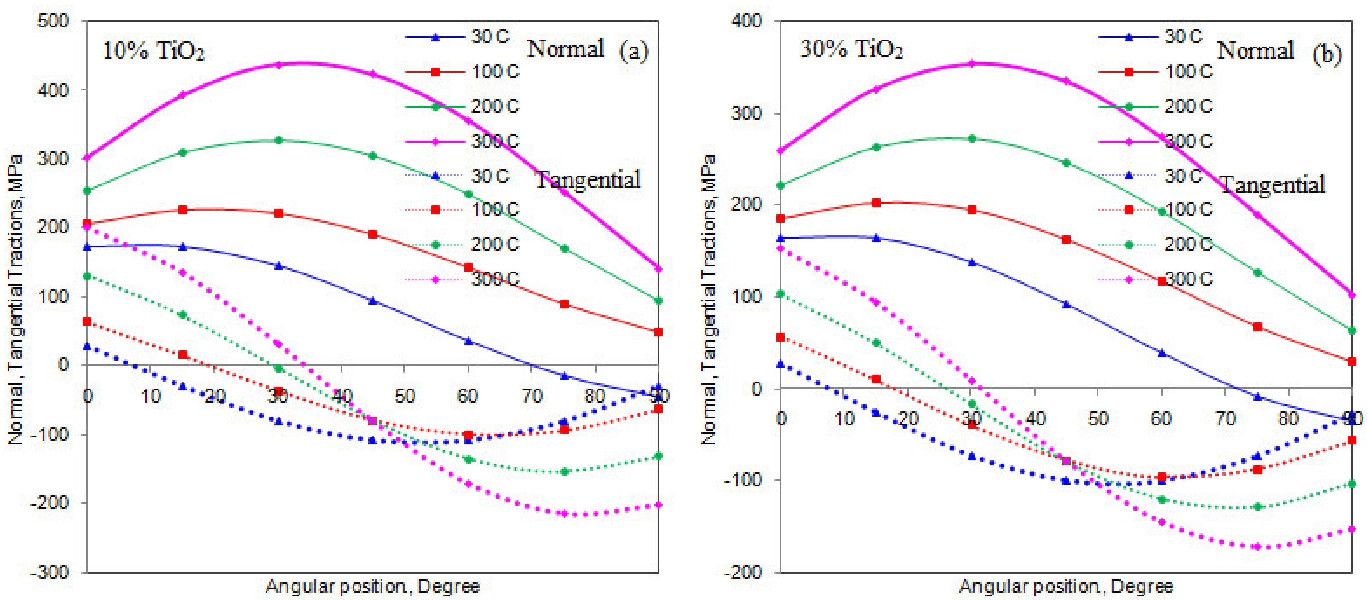

Figure 7: Normal and tangential tractions along the interphase.

The von Mises stress as a function of temperature is illustrated in figure 8. The von Mises stresses induced at the interface are higher than that induced in the nanoparticle. Hence, the interphase separation has occurred between the particle and the matrix. The particle fracture was occurred in 30% TiO_2/AA3003 alloy composites above 250°C as the stress induced in the TiO_2 particle exceeds its allowable stress due to thermal shock. The scanning electron micrograph (figure 9) of 30% TiO_2/AA3003 alloy composite confirms the occurrence of particle fracture.

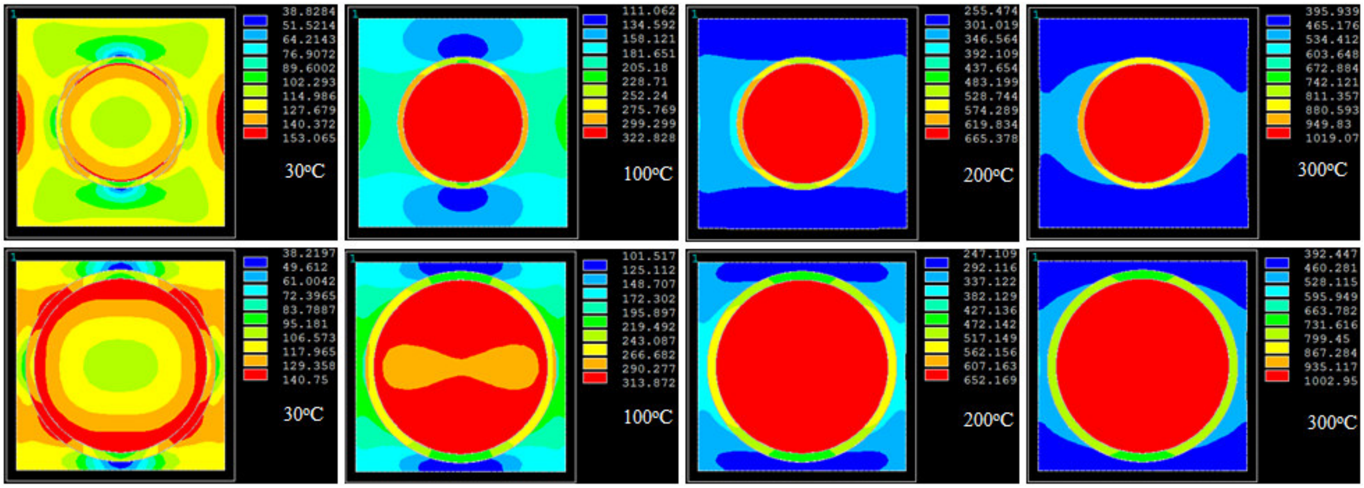

Figure 8: Images of von Mises stresses obtained from FEA: (a) 10% TiO_2/AA3003 alloy and (b) 30% TiO_2/AA3003 alloy composites.

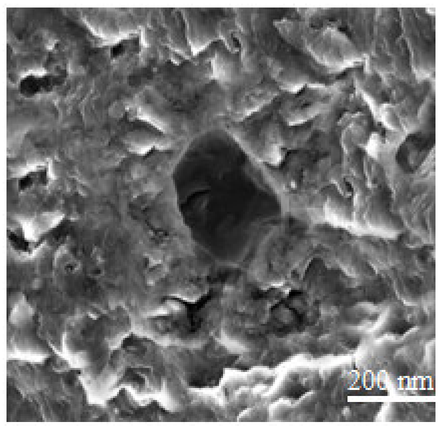

Figure 9: SEM illustrating the interphase separation.

4. CONCLUSION

The microstructure of TiO_2/AA3003 alloy composites reveals random uniform distribution of TiO_2 nanoparticles in AA3003 alloy. The shear stress is high at the interface resulting to interphase separation from the particle and the matrix. The interphase separation has occurred between the particle and the matrix. The particle fracture has occurred in 30% TiO_2/AA3003 above 250°C.

REFERENCES

1. T. Mori, K. Tanaka, Acta Metallurgica, Average Stress in Matrix and Average Elastic Energy of Materials with Misfitting Inclusions, 21, 1973, pp. 571–574.
2. A. Chennakesava Reddy, Evaluation of Debonding and Dislocation Occurrences in Rhombus Silicon Nitride Particulate/AA4015 Alloy Metal Matrix Composites, 1st National Conference on Modern Materials and Manufacturing, Pune, India, 19-20 December 1997, pp. 278-282.
3. A. Chennakesava Reddy, Interfacial Debonding Analysis in Terms of Interfacial Tractions for Titanium Boride/AA3003 Alloy Metal Matrix Composites, 1st National Conference on Modern Materials and Manufacturing , Pune, 19-20 December, 1997.
4. A. Chennakesava Reddy, Assessment of Debonding and Particulate Fracture Occurrences in Circular Silicon Nitride Particulate/AA5050 Alloy Metal Matrix Composites , National Conference on Materials and Manufacturing Processes, Hyderabad, India, 27-28 February 1998, pp. 104-109.
5. A. Chennakesava Reddy, Local Stress Differential for Particulate Fracture in AA2024/Titanium Carbide Nanoparticulate Metal Matrix Composites, National Conference on Materials and Manufacturing Processes, Hyderabad, India, 27-28 February 1998, pp. 127-131.

6. A. Chennakesava Reddy, Micromechanical Modelling of Interfacial Debonding in AA1100/Graphite Nanoparticulate Reinforced Metal Matrix Composites, 2nd International Conference on Composite Materials and Characterization, Nagpur, India, 9-10 April 1999, pp. 249-253.
7. A. Chennakesava Reddy, Cohesive Zone Finite Element Analysis to Envisage Interface Debonding in AA7020/Titanium Oxide Nano-particulate Metal Matrix Composites, 2nd International Conference on Composite Materials and Characterization, Nagpur, India, 9-10 April 1999, pp. 204-209.
8. H. B. Niranjan, A. Chennakesava Reddy, Computational Modeling of Interfacial Debonding in Fused Silica/AA7020 Alloy Particle-Reinforced Metal Matrix Composites, 3rd International Conference on Composite Materials and Characterization, Chennai, India, 11-12 May 2001, pp. 222-227.
9. H. B. Niranjan, A. Chennakesava Reddy, Nanoscale Characterization of Interfacial Debonding and Matrix Damage in Titanium Carbide/AA8090 Alloy Particle-Reinforced Metal Matrix Composites, 3rd International Conference on Composite Materials and Characterization, Chennai, India, 11-12 May 2001, pp. 228-233.
10. S. Sundara Rajan, A. Chennakesava Reddy, Assessment of Temperature Induced Fracture in Boron Nitride/AA1100 Alloy Particle-Reinforced Metal Matrix Composites, 3rd International Conference on Composite Materials and Characterization, Chennai, India, 11-12 May 2001, pp. 234-239.
11. S. Sundara Rajan, A. Chennakesava Reddy, Estimation of Fracture in Zirconia/AA2024 Alloy Particle-Reinforced Composites Subjected to Thermo-Mechanical Loading, 3rd International Conference on Composite Materials and Characterization, Chennai, India, 11-12 May 2001, pp. 240-245.
12. P. M. Jebaraj, A. Chennakesava Reddy, Finite Element Predictions for the Thermoelastic Properties and Interphase Fracture of Titanium Nitride /AA3003 Alloy Particle-Reinforced Composites, 3rd International Conference on Composite Materials and Characterization, Chennai, India, 11-12 May 2001, pp. 246-251.
13. P. M. Jebaraj, A. Chennakesava Reddy, Effect of Thermo-Mechanical Loading on Interphase and Particle Fractures of Titanium Oxide /AA4015 Alloy Particle-Reinforced Composites, 3rd International Conference on Composite Materials and Characterization, Chennai, India, 11-12 May 2001, pp. 252-256.
14. A. Chennakesava Reddy, Effect of CTE and Stiffness Mismatches on Interphase and Particle Fractures of Zirconium Carbide /AA5050 Alloy Particle-Reinforced Composites, 3rd International Conference on Composite Materials and Characterization, Chennai, India, 11-12 May 2001, pp. 257-262.
15. A. Chennakesava Reddy, Behavioral Characteristics of Graphite /AA6061 Alloy Particle-Reinforced Metal Matrix Composites, 3rd International Conference on Composite Materials and Characterization, Chennai, India, 11-12 May 2001, pp. 263-269.
16. X.A. Zhong, W.G. Knauss, Analysis of interfacial failure in particle-filled elastomers, Journal of Engineering Materials and Technology 119, 1997, pp. 198–204.